Hindawi
Journal of Sensors
Volume 2019, Article ID 9614630, 10 pages
https://doi.org/10.1155/2019/9614630

*Research Article*

# A Real-Valued Genetic Algorithm for Optimization of Sensor Placement for Guided Wave-Based Structural Health Monitoring

**Rohan Soman and Pawel Malinowski**

*Institute of Fluid Flow Machinery, Polish Academy of Sciences, 14 Fiszera Street, Gdansk 80-231, Poland*

Correspondence should be addressed to Rohan Soman; rsoman@imp.gda.pl

Received 13 August 2019; Accepted 5 November 2019; Published 10 December 2019

Academic Editor: Antonio Lazaro



The paper presents a novel implementation of the genetic algorithm (GA) to improve the coverage of the sensor network for damage detection using guided waves. The implementation allows depiction of sensor locations with real values which is closer to the real-life situation. Also, additional features such as proximity checks and node insertions have been implemented in order to improve the convergence of the GA as well as the thoroughness of the search space. For the traditional integer-based implementation, the size of the problem is large but finite. For the real-valued implementation, the problem size can indeed be infinitely large. So added measures have been introduced such as a two-step optimization process for the reduction in size and improved convergence.

## 1. Introduction

Guided wave- (GW) based structural health monitoring (SHM) in one of the most widely used techniques for large plate or pipe-like structures. The propagating wave may be used to cover a large area and through the processing of the time of flight (TOF) allows damage isolation. The GW have been shown to be sensitive to extremely small levels of damage and have been employed for detection of damage due to impact, corrosion, and fatigue [1–4].

The research in the area of GW in metallic structures is quite extensive, but the work in the area of sensor placement is quite limited. Ostachowicz et al. [5] present an excellent review of the techniques used in the optimization of sensor placement with a special section dedicated to the optimization of sensor placement for GW-based SHM. The literature can be divided into primarily 3 areas. The first work in the area of sensor placement optimization was based on improving the probability of detection (POD). Staszewski et al. [6] used it in conjunction with artificial neural networks for improving the probability of impact localization and detection. Markmiller and Chang [7] used a metric dependent on the POD which was computed based on the response reconstruction of the impact event. Staszewski et al. and Markmiller et al. both used GA for the optimization. Flynn and Todd [8] used the probabilistic approach as well in the form of Bayes' risk. The aim is to minimize the false-positive and false-negative errors caused by the sensor network. Haynes [9] built on the Bayes' risk framework and included the cost of the SHM system in the decision-making process. Similar approaches based on the false alarms were also proposed by Vanli et al. [10] and Coelho et al. [11].

The second philosophy of the optimization is to improve the sensitivity of the network to damage. The work done in this area is largely finite element model based, where different damage scenarios are numerically simulated and used to determine the sensor locations such as the one by Lee and Staszewski [12]. Venkat et al. [13] and Ewald et al. [14] also present a method for locating the sensors at the maxima of the differential image of the healthy and damaged condition of the structure. These methods are useful for optimization of placement for the known hotspots in the structure.

Another philosophy of the optimization is to maximize the coverage of the sensor network. Soni et al. [15] developed a sensor placement algorithm based on the minimal sensing distance. The sensing range was determined based on the

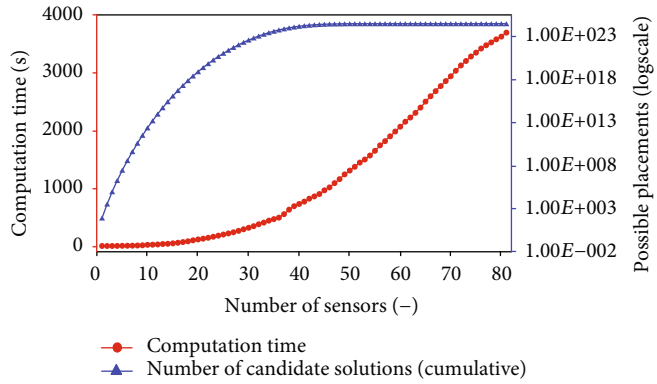


Figure 1: Problem size and computation time for increasing number of sensors.

signal to noise ratio (SNR) and the attenuation of the waves. The minimum sensor range was a circle of fixed radius determined experimentally. The backward sequential sensor placement (BSSP) was used in order to remove the redundant sensors in the network. Coelho et al. also developed an approach based on maximizing the coverage area by minimizing the probability of false alarms. Thiene et al. [16] proposed maximizing of coverage area based on a pixelated approach. The sample of interest was divided into pixels, and the coverage of the sensor network was calculated for each pixel. The different wave propagation features such as attenuation, line of sight, and shape of the sample can be incorporated based on different multiplication factors for obtaining the fitness function. The number of candidate locations are restricted in the study in order to limit the problem size. But this unnatural constraint may limit the performance of the optimization algorithm. The number of possible sensor locations was increased by Soman et al. [17] through the use of an analytical approach which is computationally more efficient than the pixel-based approach. Soman et al. [17] then extended the optimization cost function also to improve the quality of the damage isolation. The damage isolation in the GW-based SHM is carried out by the triangulation technique. Soman et al. included the area covered by at least 3 sensors as an additional metric. The multiobjective optimization problem was scalarized using weighing functions in order to simplify the optimization using the GA. Tarhini et al. [18] too used coverage of the specimen as a optimization objective. They developed a mixed integer nonlinear program which does not constrain the optimization search to a limited number of possible sensor locations and is a motivation for the current research.

In the present paper, the authors build on the defined cost function with 3 optimization objectives, namely, coverage by at least 1 sensor-actuator pair, coverage by 3 sensor-actuator pairs and the number of sensors. The implementation of the GA is changed from an integer GA to a real-valued GA. In order to restrict the size of the optimization problem, the number of sensors is limited to a range of values. This range is determined based on the sensor densities required for the SNR to allow reliable damage detection. The cost function computation is the most computationally demanding step, and hence, the number of unnecessary computations needs to be reduced. In order to limit this number, some features such as node insertion and the proximity detection have been added to the implementation.

The rest of the paper is organized as follows: the next section explains the methodology for defining the optimization problem. Section 3 presents the additional functionalities such as node insertion and proximity check implemented for improving the performance of the GA. Section 4 covers the results of the optimization and the comparison of the improved GA with the earlier work. The last section draws some conclusions and presents areas of future work.

## 2. Methodology

The increase in number of sensors deployed on a structure leads to an increase in the deployment costs as well as secondary costs related to the extra weight of the sensors and the wiring as well as the processing and storage of the data. Hence, one of the objectives of the optimization of sensor placement should be the minimization of sensors used. This minimization can be implemented in the cost function or as a constraint in the allowed placements. If it is incorporated in the cost function as by Soman et al. [17], the number of possible sensor placements increases. The optimization problem becomes very large, and as a result, the time needed for convergence is very large. Also, the time consumed for the computation of the cost function increases with the increase in number of sensors as shown in Figure 1. The computations are based on the implementation of the GA reported in [17].

Also, the sensor placements with the large number of sensors are not feasible due to the availability of the resources. Thus, in order to reduce the size of the optimization problem, constraints on the number of sensors may be imposed right at the implementation stage. This constraint must be imposed in an objective way in order to ensure that the sensor performance is within the acceptable range. Thus, this section discusses a formal method for determining the maximum number of sensors.

*2.1. Sensor Number Determination.* The number of sensors is determined based on sensor densities using the concept developed by Croxford et al. [19]. They provide an excellent discussion and step by step process for calculating the different parameters for determining the sensor densities. For completeness, the equations for calculating the sensor pitch

and all the factors are provided here without the derivation which can be found in [19]. The minimum pitch of the sensors is given by

$$p = \left( \frac{3^{3/4} R_{\text{damage}}}{\sqrt{2} S \beta \delta T} \right)^{(2/3)}, \quad (1)$$

where $R_{\text{damage}}$ is the reflection coefficient of the damage (defined in terms of the scattered wave amplitude at unit distance from the damage), $S$ is the minimum SNR required for reliable damage assessment, $\beta$ is the coefficient corresponding to the post subtraction noise between the baseline signal and the signal at the present time, and $\delta T$ is the change in temperature. The factor $\beta$ is dependent on the type of subtraction carried out as well as the wave mode. In the paper by Croxford et al., the value for RF subtraction is given by

$$\beta_{\text{RF}} = 2\pi f \frac{1}{v_{\text{ph}}} \left( \alpha - \frac{k_{\text{ph}}}{v_{\text{ph}}} \right), \quad (2)$$

where $v_{\text{ph}}$ is the phase velocity, $k_{\text{ph}}$ is the coefficient relating the sensitivity of the phase velocity to temperature, and $\alpha$ is the coefficient of expansion.

The factor $R_{\text{damage}}$ is dependent on the type of damage considered. For a hole in the plate considered as a cylindrical scatterer, the coefficient can be analytically given by

$$R_{\text{damage}} = 0.55\sqrt{d}, \quad (3)$$

where $d$ is the diameter of the hole in m.

Knowing the values for all the parameters in equation (1), the pitch of sensors can be calculated which in turn may be used for determining the minimum number of sensors. The maximum number of sensors then can be determined by introducing some redundancy in the system. As shown in Figure 1, the problem size and the computation time increase with the increase in the maximum number of sensors. So care should be taken in defining the maximum number. For the purpose of the study and to ensure some redundancy, the maximum number of sensors was identified as 50% more than the minimum number of sensors required.

The sample of interest was an aluminium plate with dimensions 1 m × 1 m × 1 mm shown in Figure 2. Added mass was used to simulate damage. The backscatter profile of the added mass was obtained based on the full-field measurements from the laser Doppler vibrometer as shown in Figure 3. The result is for the centrally located mass shown in Figure 2.

As can be seen, the minimum value for the backscatter was 0.073 which is taken as the back-scatter $R_{\text{damage}}$. Key points to note is that the backscatter is more or less symmetrical (within reasonable errors). The small error can be attributed to the fact that the sampled points were in a rectangular grid as opposed to a radial grid. Hence, the distances at the point of measurement were approximately equal. The maximum backscatter occurs at 45° to the incident angle. The

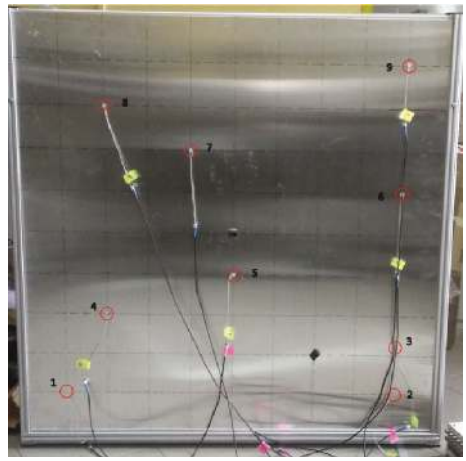

Figure 2: Aluminium plate under investigation [17].

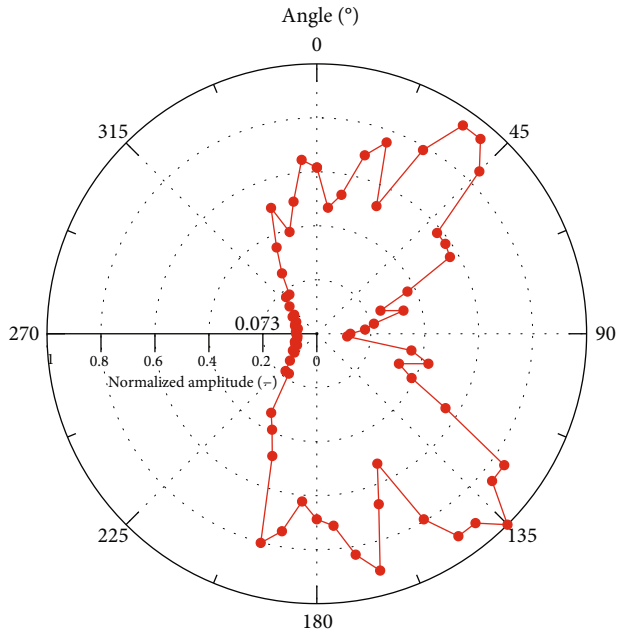


Figure 3: Backscatter of the waves due to discontinuity (added mass)—excitation from 90°.

minimum value is in the area just beyond the mass as is expected. So the worst case will be when the sensor is at the other side of the actuator which is considered in computing the minimum number of sensors. The backscattering index obtained is equivalent to 17 mm hole in the sample according to equation (3) which is a reasonable assumption for a scattering object. The $\beta$ value for the aluminium plate S0 wave based on equation (2) is given as 0.0962. In the author's team, methods have been developed for temperature compensation which allow -14 dB change in the SNR for 10°C change in temperature [20]. The 14 dB change results in $\beta = 0.0192$. The SNR = 2 (similar to [19]) has been assumed to be necessary for ensuring reliable damage detection. Based on these inputs, the $p$ calculated based on equation (1) is 0.454 which relates to the minimum number of sensors as 6. Taking into

consideration the proposed redundancy in the system, the maximum number of sensors is calculated as 9. This allows comparison of the method with the older method as the sensor optimization carried out previously and reported in [17] was on a network of 9 sensors.

*2.2. Sensor Location Optimization.* Once the number of sensors is known, an optimization scheme can be implemented by restricting the number of sensors between the lower and the upper limits. The criterion for the optimization is given by the cost function. As has been mentioned in [17], the three demands from the application are as follows:

(1) coverage with at least 1 sensor-actuator pair (coverage1)

(2) coverage with at least 3 sensor-actuator pairs (coverage3)

(3) number of sensors ($s$)

Based on these demands, a scalarized cost function can be developed by using weighing factors as shown in

$$\text{cost} = -1 \times \left( \omega \frac{\text{coverage3}}{s^{\gamma}} + (1-\omega) \frac{\text{coverage1}}{s^{\delta}} \right), \quad (4)$$

where coverage3 is the % of points of the grid which lie within the sensing range of 3 or more sensor-actuator pairs; coverage1 is the % of points which lie in the sensing range of a single sensor-actuator pair. $\omega$, $\gamma$, and $\delta$ are weighting values to determine the relative merit for each of the parameters, and $s$ is the number of sensors. The parameters $\gamma$ and $\delta$ can be treated as independent of each other or dependent based on the choice. The two parameters were introduced to show the different correlations of the coverage3 and coverage1 values to the number of sensors.

For the two-stage optimization implementation illustrated in this paper, the choice of the weighing parameters is even more sensitive. As the change in the number of sensors is limited, the range of values for the parameter too are limited and do not show much change. Hence if the weighing values for $\gamma$ and $\delta$ are too low (e.g., 0), the algorithm will choose solutions with maximum number of sensors while if they are too high (e.g., 1), the number of sensors will have a very high bearing on the sensor placement, and as such, the placements with lower number of sensors will be preferred. This value depends on the contribution of each sensor to the coverage of the network. For metallic structure without any structural features such as stiffeners, each sensor contributes significantly; hence, the low values for $\gamma$ and $\delta$ need to be chosen. Sensitivity studies were carried out with evenly spaced sensor placements (Figure 4) for different number of sensors as shown in Table 1. It is acknowledged that the evenly spaced sensor placements may or may not be optimal. The aim of Table 1 and Figure 4 is to show the contribution of each sensor towards the coverage1 and coverage3 values and their bearing on the choice of $\gamma$ and $\delta$ values.

As can be seen in Table 1, the contribution per sensor reduces but the overall coverage increases with the increase in the sensor number. In order to obtain similar cost for sensor placement with 6 sensors and 9 sensors, the $\delta$ value needs to be 0.17. Similarly, the $\gamma$ value needs to be 0.26. As mentioned, the evenly placed sensor placement is suboptimal; as a result, the sensor contribution too is suboptimal. For optimized sensor placements, the values for $\gamma$ and $\delta$ should be significantly lower. Hence, for the purpose of the study, values of $\gamma$ and $\delta$ were taken as 0.15.

The optimization of the locations was carried out using a real-valued implementation of the GA with special tools and routines incorporated for improved convergence which have been described in the next section.

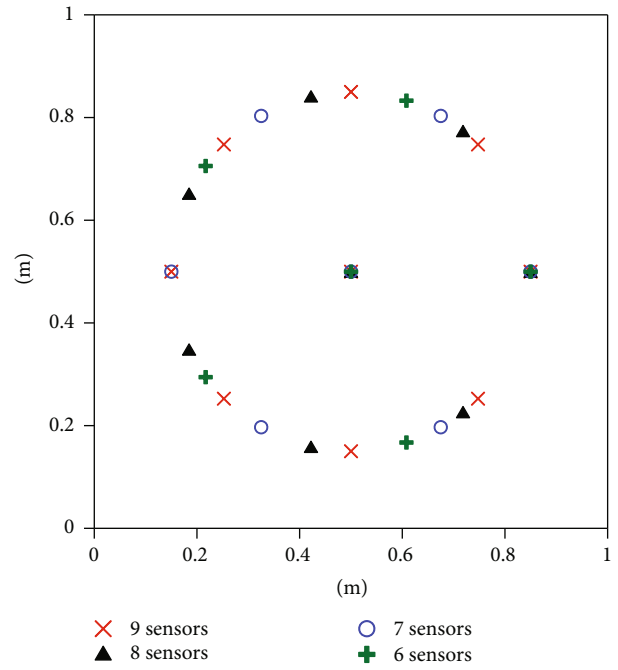


Figure 4: Even distribution of sensors to show sensor contribution.

Table 1: Change in metrics with different number of evenly distributed sensors.

| $s$ | coverage1 % | coverage3 % | Contribution per sensor to coverage1 % | % contribution per sensor to coverage3 % |
|---|---|---|---|---|
| 6 | 84.1 | 74.5 | 14.0 | 12.4 |
| 7 | 85.2 | 77.4 | 12.2 | 11.1 |
| 8 | 86.6 | 78.5 | 10.8 | 9.8 |
| 9 | 90.2 | 82.8 | 10.0 | 9.2 |

## 3. Implementation of the GA

The main innovation of the paper is the implementation of real-valued GA as opposed to the commonly used integer GA for sensor placement optimization. The underlying motivation for this is the observation that the more realistic the encoding of the optimization, the better the performance of

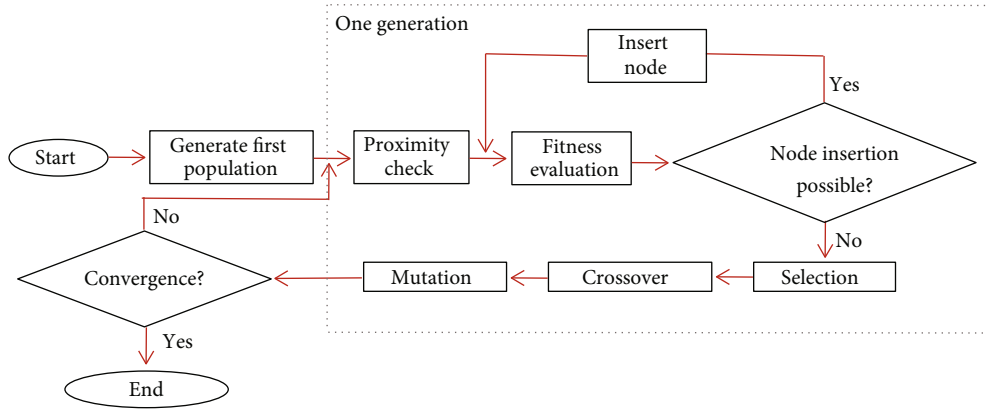


Figure 5: GA flowchart.

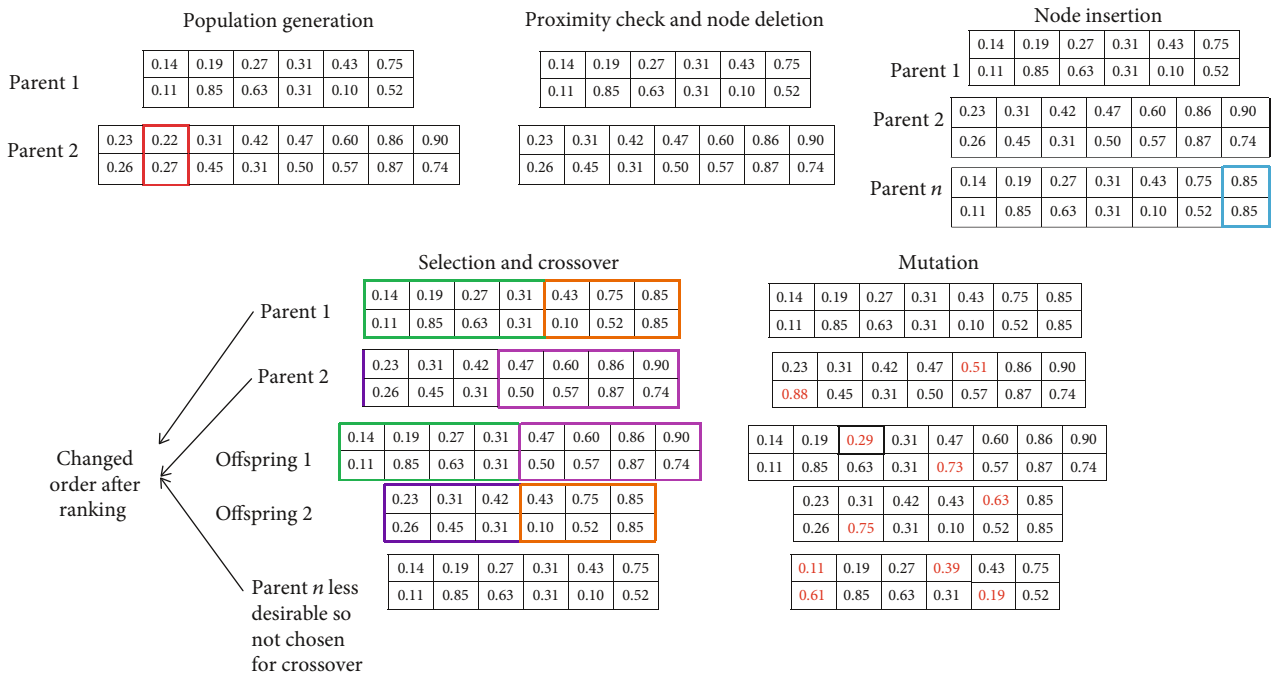


Figure 6: Example of the real-encoded GA with additional features.

the algorithm. Also, by changing the implementation from the integer to real GA, the difference in the phenotype for a unit change in the sensor values is significantly reduced thus allowing better search in the sample space. On the downside, the size of the problem is no longer finite but infinite. Thus, there is no way for checking the validity of the optimization tool with brute-force methods. The flow chart for the GA is provided in Figure 5.

The population is generated with each individual sensor placement depicted by $2 \times N$. The first row corresponds to the $x$-coordinate while the second row corresponds to the $y$-coordinate. The $x$ and $y$ coordinates are treated as independent in the population generation, fitness evaluation, node insertion, and mutation phases while in the crossover and selection phase, $y$-coordinate is treated as dependent variable. The number $N$ corresponds to number of sensors and can take any value in the chosen range determined by the method outlined in Section 2.1. The different features incorporated in the GA are shown through an example in Figure 6.

*3.1. Proximity Check.* This feature is introduced to avoid concentration of the nodes at a point or ensure the feasibility of the sensor placement. In the first step, nodes which are too close to the boundaries are omitted as it will be difficult to

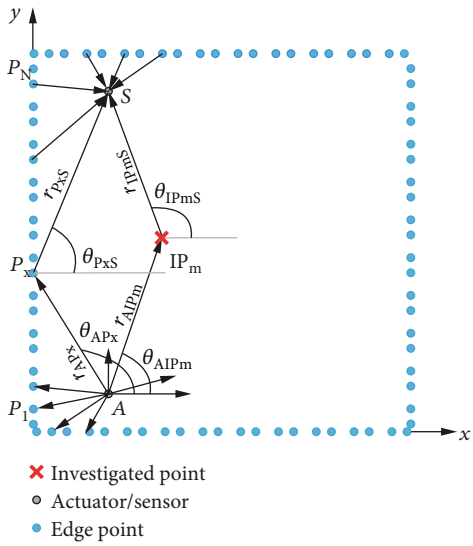


Figure 7: Schematic explaining the ray-tracing approach.

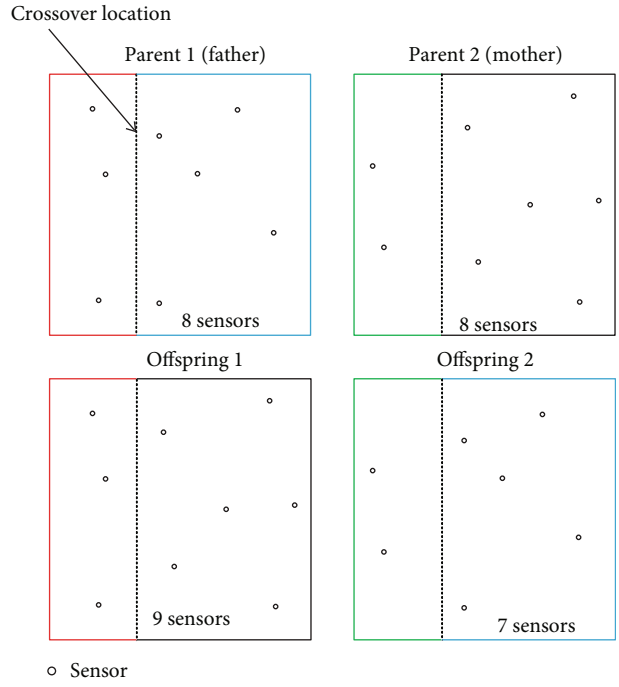


Figure 8: Mirror crossover schematic.

distinguish between direct signals and the reflection from the boundary. In the next stage, redundancy in the system because of 2 closely spaced sensors is reduced by deleting the sensor. The limit for the proximity check was taken as the diameter of the sensors used which was 0.01 m. This constraint ensures that the optimized network is possible to be realized physically.

*3.2. Node Insertion.* In case the proximity check removes a gene from the chromosome, there is a possibility to increase the number of sensor in the chromosome by adding a node at the location with the poorest coverage. The node is inserted if it provides an advantage over the existing sensor placement in terms of the coverage3, coverage1, and the scalarized cost function. The node insertion is repeated until the insertion is possible and desirable. The chromosome with the added gene replaces the lowest ranked chromosome in the selection process. The node insertion allows a better local search but at the cost of possible entrapment in the local minima. This entrapment is caused as there are two copies of very similar chromosomes which are very desirable in the population. So in order to avoid their domination in the subsequent generations, the number of chromosomes in each generation is increased as compared to the previous implementation of the GA reported in [17].

*3.3. Fitness Evaluation.* In the previous work by the authors, the analytical approach based on the largest ellipse fitting inside the plate was employed for determining the coverage of each sensor-actuator pair. This approach is simple to implement for simple structures and is computationally efficient. For problems where the propagation is direction dependent (anisotropic structures, or structures with damage backscatter with an angle-dependent profile), the ellipse approach is not valid. Hence, the ray-tracing approach [21] explained in Figure 7 was employed. In the ray-tracing approach, a ray is extended from the actuator to the location under investigation and another ray is extended between the investigated point and the sensor. The attenuation, velocity, or backscatter can be incorporated based on the angle of the rays with the coordinate axes and the distance between the points. The maximum allowed TOF is determined from the edge points. This TOF is then used to construct a limiting ellipse with the major axis equal to the product of maximum velocity and the TOF. The points within the ellipse are then checked individually with the ray-tracing approach to determine the coverage of the sensor-actuator pair. The fitness value evaluated for the sensor network is the superposition of the coverage for each sensor-actuator pair.

*3.4. Crossover.* The standard crossover techniques used in the GA are the single-point crossover, the multipoint crossover, the arithmetic crossover, etc. [22]. They are simplistic to implement but often are not exactly aligned with the implementation and the physical nature of the problem. As mentioned earlier, the closer the encoding of the problem to reality, the better is the performance of the optimization. Hence, the mirror crossover [23] was implemented for the optimization problem. The method for the mirror crossover is shown in Figure 8 and is as follows: two parents are selected randomly similarly to the other crossover techniques.

Then, a random value $x_{cross}$ of the $x$-coordinate is generated. All genes with $x > x_{cross}$ in the father are transferred to offspring 1 and $x \leq x_{cross}$ in the father to offspring 2. The genes with $x > x_{cross}$ from the mother are transferred to offspring 1 and $x \leq x_{cross}$ from the mother are transferred to offspring 2.

As can be seen, the number of sensors in both parents is 8. By the use of mirror crossover, it is possible to obtain a sensor placement with fewer number of sensors (7 in

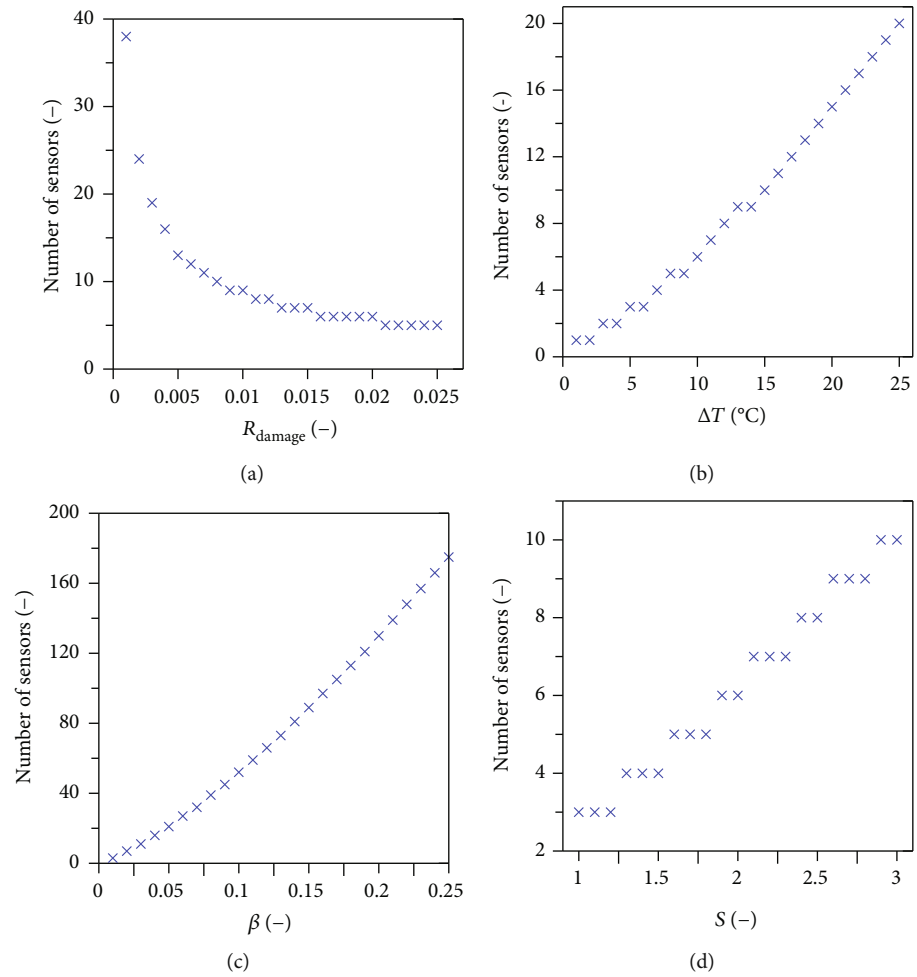


Figure 9: Change in minimum number of sensors with different parameters: (a) $R_{damage}$; (b) $\Delta T$; (c) $\beta$; (d) $S$.

offspring 2). Thus, increasing the search capability of the optimization algorithm.

*3.5. Algorithm Inputs.* For obtaining the optimized sensor placement, several variables need to be determined based on the sensitivity analysis. For the problem size at hand, the number of chromosomes was taken as 256. This is to minimize the domination of the gene pool by a few genes due to the node insertion phase. The elitism was 50%. The mutation rate was 25%, and number of generations was 5000. The next section compares the results of the optimization from the real-valued GA with the integer GA.

## 4. Results and Discussion

*4.1. Sensor Number.* As shown in Section 2, the pitch of the sensors and in turn the sensor density is dependent on the values of $R_{damage}$, $S$, $\beta$, and $\Delta T$. The parameter $R_{damage}$ depends on the backscatter characteristics of the damage while the parameter $\beta$ depends on the material and the central frequency used for the excitation. Figure 9 shows the change in the number of sensors with unilateral change in any of the 4 variables.

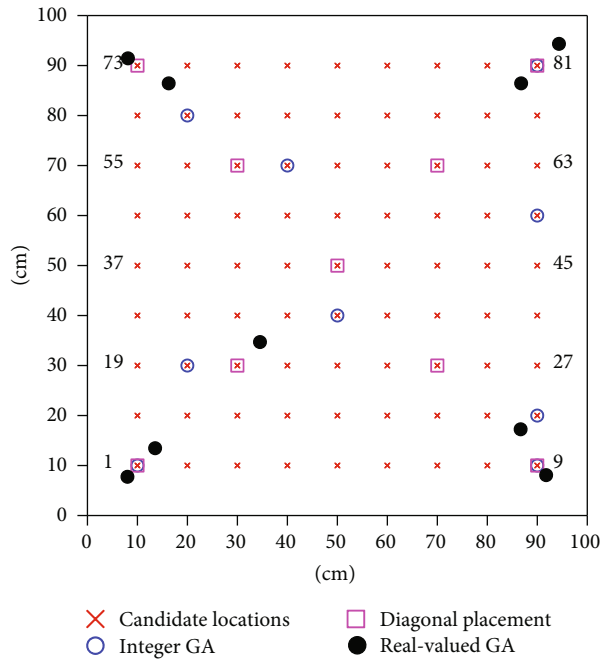


Figure 10: Sensor placement for different runs.

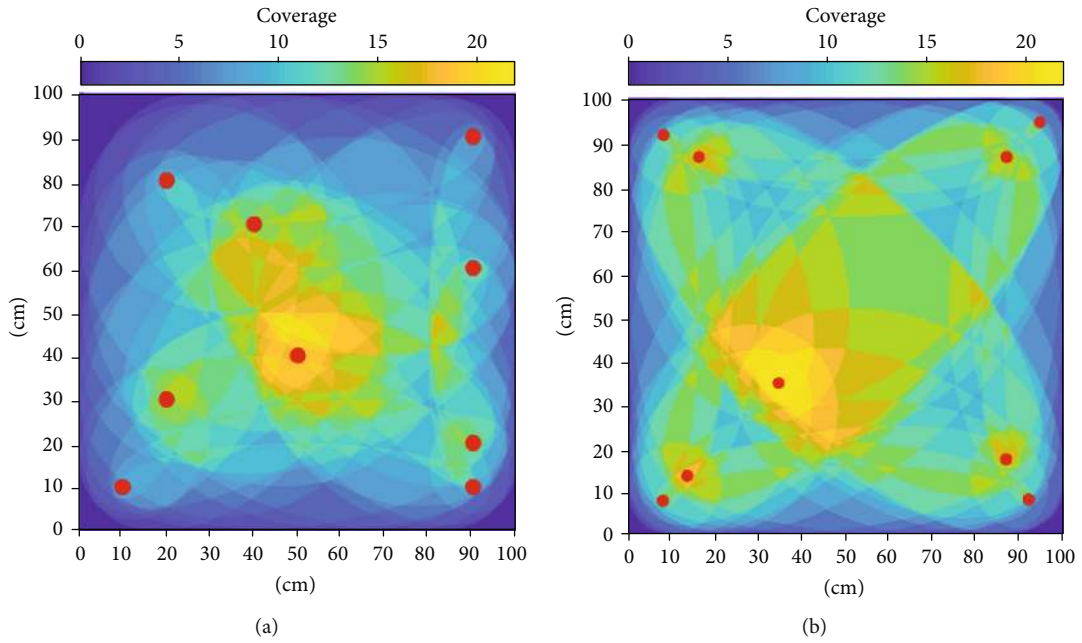


Figure 11: Surface plot showing coverage: (a) integer GA-based placement; (b) real GA-based placement.

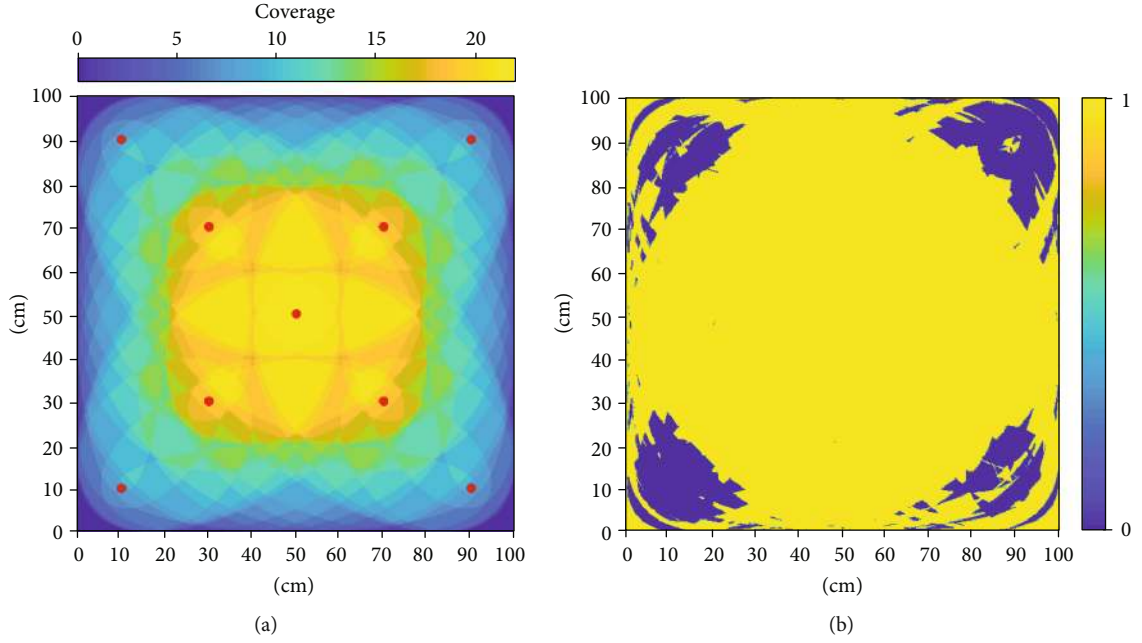


Figure 12: Surface plot showing coverage: (a) diagonal placement; (b) difference in coverage for real-coded GA and diagonal placement (yellow shows area with improvement).

The factor $R_{\text{damage}}$ can be changed with the size and type of defect which is to be detected. The factor $\Delta T$ depends on the uncertainty in ambient conditions expected during the application. The value of $\beta$ depends on the frequency of excitation as well as the material properties. The material properties affect the phase and group velocity as well as the dependence of the material on the change in temperature. The factor $S$ depends on the quality of the signal processing and noise cancellation algorithm. It can also be used to introduce the effects of attenuation which is significant in composites. The value of $S$ can be increased in case the attenuation is high in order to determine the sensor density.

*4.2. Sensor Location.* The real-valued implementation of the optimization eliminates the unnecessary constraint on the locations of sensors imposed due to the integer-based implementation. As a result, better coverage3 and coverage1 and in turn better fitness value may be achieved. Figure 10 shows the

Table 2: Performance parameters for different sensor placements.

| Run | Generations | coverage1 | coverage3 |
|---|---|---|---|
| Integer GA | 5000 | 96.1% | 88.7% |
| Real GA | 5000 | 98.2% | 96.0% |
| Diagonal | — | 97.7% | 94.8% |

optimal sensor placement achieved for the integer placement and for the real-valued optimization. Figures 11(a), 11(b), and 12(a) show the coverage plot for the three sensor placements. Figure 12(b) also shows the improved coverage achieved through the real-valued implementation. The objective values for the optimization are quantitatively compared in Table 2.

## 5. Conclusions

The paper outlines a two-step methodology for optimization of sensor placement for GW-based damage detection. In the first step, the minimum number of sensors needed is calculated based on the quality of the signal processing algorithm. Once the number of sensors is determined, the location of the sensors is optimized through improved implementation of the GA. The optimization problem is posed using real values rather than constraining the search with the use of integer-based implementation. In order to account for the increase in the search space for optimal solution and improve the computational performance of the algorithm, some key features have been introduced in the GA such as proximity checking, node insertion, and use of mirror crossover scheme. The use of these features allows the improvement in the search capability as well as the computational efficiency of the search algorithm.

The paper presents sensitivity studies for the different parameters in determining the number of sensors. The paper also shows that through the use of real-valued implementation improved coverage using the same number of sensors can be achieved. Also, the computational efficiency for the real-valued GA is better than the integer GA. Based on the presented results, the use of real-valued GA is recommended. Incorporation of backscatter profiles from different damage scenarios, use of the technique for composite structures with structural features such as stiffener, rivets, and the experimental validation of the proposed methodology are identified as the areas of further research.

## Data Availability

The raw/processed data required to reproduce these findings cannot be shared at this time as the data also forms part of an ongoing study.

## Disclosure

The opinions expressed in this paper do not necessarily reflect those of the sponsors.

## Conflicts of Interest

The authors declare no conflict of interest.

## Authors' Contributions

The conceptualization, methodology, validation, optimization, writing, review and editing, and visualization for the manuscript were carried out by R.S. The resources, LDV measurements and data processing, supervision, project administration, and funding acquisition were carried out by P.M.

## Acknowledgments

The authors are grateful to TASK-CI for allowing the use of their computational resources. This research was funded by the National Science Center, Poland, under the Sonata-Bis 6 call with the grant number: 2016/22/E/ST8/00068.

## References

[1] M. Salmanpour, Z. Sharif Khodaei, and M. Aliabadi, "Impact damage localisation with piezoelectric sensors under operational and environmental conditions," *Sensors*, vol. 17, no. 5, p. 1178, 2017.

[2] J. He, Y. Ran, B. Liu, J. Yang, and X. Guan, "A fatigue crack size evaluation method based on lamb wave simulation and limited experimental data," *Sensors*, vol. 17, no. 9, p. 2097, 2017.

[3] S. Sikdar and S. Banerjee, "Identification of disbond and high density core region in a honeycomb composite sandwich structure using ultrasonic guided waves," *Composite Structures*, vol. 152, pp. 568–578, 2016.

[4] W. Li, C. Xu, and Y. Cho, "Characterization of degradation progressive in composite laminates subjected to thermal fatigue and moisture diffusion by lamb waves," *Sensors*, vol. 16, no. 2, p. 260, 2016.

[5] W. Ostachowicz, R. Soman, and P. Malinowski, "Optimization of sensor placement for structural health monitoring: a review," *Structural Health Monitoring*, vol. 18, no. 3, pp. 963–988, 2019.

[6] W. J. Staszewski, K. Worden, R. Wardle, and G. R. Tomlinson, "Fail-safe sensor distributions for impact detection in composite materials," *Smart Materials and Structures*, vol. 9, no. 3, pp. 298–303, 2000.

[7] J. F. Markmiller and F.-K. Chang, "Sensor network optimization for a passive sensing impact detection technique," *Structural Health Monitoring*, vol. 9, no. 1, pp. 25–39, 2010.

[8] E. B. Flynn and M. D. Todd, "Optimal placement of piezoelectric actuators and sensors for detecting damage in plate structures," *Journal of Intelligent Material Systems and Structures*, vol. 21, no. 3, pp. 265–274, 2010.

[9] C. M. Haynes, *Effective health monitoring strategies for complex structures, [Ph.D. thesis]*, UC San Diego, 2014.

[10] O. A. Vanli, C. Zhang, A. Nguyen, and B. Wang, "A minimax sensor placement approach for damage detection in composite structures," *Journal of Intelligent Material Systems and Structures*, vol. 23, no. 8, pp. 919–932, 2012.

[11] C. K. Coelho, S. B. Kim, and A. Chattopadhyay, "Optimal sensor placement for active guided wave interrogation of complex

metallic components," in *Sensors and Smart Structures Technologies for Civil, Mechanical, and Aerospace Systems 2011*, vol. 7981, p. 79813O, San Diego, CA, USA, 2011.

[12] B. Lee and W. Staszewski, "Sensor location studies for damage detection with lamb waves," *Smart Materials and Structures*, vol. 16, no. 2, pp. 399–408, 2007.

[13] R. S. Venkat, C. Boller, N. Ravi et al., "Optimized actuator/sensor combinations for structural health monitoring: simulation and experimental validation," in *Structural Health Monitoring 2015*, Stanford, USA, 2015.

[14] V. Ewald, R. M. Groves, and R. Benedictus, "Transducer placement option of lamb wave SHM system for hotspot damage monitoring," *Aerospace*, vol. 5, no. 2, p. 39, 2018.

[15] S. Soni, S. Das, and A. Chattopadhyay, "Optimal sensor placement for damage detection in complex structures," in *Volume 2: Multifunctional Materials; Enabling Technologies and Integrated System Design; Structural Health Monitoring/NDE; Bio-Inspired Smart Materials and Structures*, pp. 565–571, Oxnard, CA, USA, 2009.

[16] M. Thiene, Z. S. Khodaei, and M. Aliabadi, "Optimal sensor placement for maximum area coverage (MAC) for damage localization in composite structures," *Smart Materials and Structures*, vol. 25, no. 9, article 095037, 2016.

[17] R. Soman, P. Kudela, K. Balasubramaniam, S. K. Singh, and P. Malinowski, "A study of sensor placement optimization problem for guided wave-based damage detection," *Sensors*, vol. 19, no. 8, p. 1856, 2019.

[18] H. Tarhini, R. Itani, M. A. Fakih, and S. Mustapha, "Optimization of piezoelectric wafer placement for structural health-monitoring applications," *Journal of Intelligent Material Systems and Structures*, vol. 29, no. 19, pp. 3758–3773, 2018.

[19] A. J. Croxford, P. D. Wilcox, B. W. Drinkwater, and G. Konstantinidis, "Strategies for guided-wave structural health monitoring," *Proceedings Mathematical, Physical and Engineering Sciences*, vol. 463, no. 2087, pp. 2961–2981, 2007.

[20] C. A. Dan and P. Kudela, "Temperature compensation methods for elastic wave based SHM," in *Recent Progress in Flow Control for Practical Flows*, P. Doerffer, G. Barakos, and M. Luczak, Eds., pp. 483–497, Springer, Cham, 2017.

[21] R. Soman, P. Kudela, and P. Malinowski, "Improved damage isolation using guided waves based on optimized sensor placement," in *Sensors and Smart Structures Technologies for Civil, Mechanical, and Aerospace Systems 2019*, vol. 10970, p. 109700B, Denver, CO, USA, 2019.

[22] A. Umbarkar and P. Sheth, "Crossover operators in genetic algorithms: a review," *ICTACT Journal on Soft Computing*, vol. 6, no. 1, pp. 1083–1092, 2015.

[23] L. Dai and B. Wang, "Sensor placement based on an improved genetic algorithm for connected confident information coverage in an area with obstacles," in *2017 IEEE 42nd Conference on Local Computer Networks (LCN)*, pp. 595–598, Singapore, 2017.